Inorganic Chemistry

Article

pubs.acs.org/IC

Magneto-Structural Correlations in a Family of $Fe^{II}Re^{IV}(CN)_2$ Single-Chain Magnets: Density Functional Theory and Ab Initio Calculations

Yi-Quan Zhang,[†,‡] Cheng-Lin Luo,[‡] Xin-Bao Wu,[‡] Bing-Wu Wang,*[,†] and Song Gao*[,†]

[†]College of Chemistry and Molecular Engineering, Peking University, Beijing 100871, P. R. China

[‡]Jiangsu Key Laboratory for NSLSCS, School of Physical Science and Technology, Nanjing Normal University, Nanjing 210023, P. R. China

ABSTRACT: Until now, the expressions of the anisotropic energy barriers Δ_ξ and Δ_A, using the uniaxial magnetic anisotropy D, the intrachain coupling strength J, and the high-spin ground state S for single-chain magnets (SCMs) in the intermediate region between the Ising and the Heisenberg limits, were unknown. To explore this relationship, we used density functional theory and ab initio methods to obtain expressions of Δ_ξ and Δ_A in terms of D, J, and S of six R_4Fe^{II}–$Re^{IV}Cl_4(CN)_2$ (R = diethylformamide (**1**), dibutylformamide (**2**), dimethylformamide (**3**), dimethylbutyramide (**4**), dimethylpropionamide (**5**), and diethylacetamide (**6**)) SCMs in the intermediate region. The Δ_A value for compounds **1**–**3** was very similar to the magnetic anisotropic energy of a single Fe^{II}, while the value of Δ_ξ was predicted using the exchange interaction of Fe^{II} with the neighboring Re^{IV}, which could be expressed as $2JS_{Re}S_{Fe}$. Similar to compounds **1**–**3**, the anisotropy energy barrier Δ_A of compounds **4** and **5** was also equal to $(D_i - E_i)S_{Fe}^2$, but the correlation energy Δ_ξ was closely equal to $2JS_{Re}S_{Fe}(\cos 98.4 - \cos 180)$ due to the reversal of the spins on the opposite Fe^{II}. For compound **6**, one unit cell of $Re^{IV}Fe^{II}$ was regarded as a domain wall since it had two different Re^{IV}–Fe^{II} couplings. Thus, the Δ_ξ of compound **6** was expressed as $4J''S_{Re1Fe1}S_{Re2Fe2}$, where J'' was the coupling constant of the neighboring unit cells of Re1Fe1 and Re2Fe2, and Δ_A was equal to the anisotropic energy barrier of one domain wall given by $D_{Re1Fe1}(S^2_{Re1Fe1} - 1/4)$.

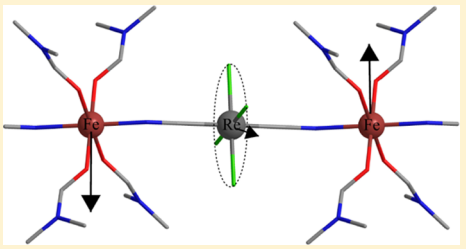

INTRODUCTION

Since Gatteschi and co-workers reported a radical-bridged one-dimensional solid of $Co(hfac)_2(NITPhOMe)$ displaying a relaxation barrier of 107 cm^{-1} in 2001,[1] single-chain magnets (SCMs) have attracted much attention in the field of molecule-based magnetic materials.[2] Many new SCMs have been reported by scientists around the world.[3−6] The relaxation barriers of these SCMs, however, are all smaller than that of the first one. Thus, it is very important to understand how to increase the energy barriers of SCMs for both experimental and theoretical chemists.

In single-molecule magnets (SMMs), the energy barrier Δ_A stems from the uniaxial magnetic anisotropy D, acting on a high-spin ground state S, such that $\Delta_A = |D|S^2$ for integer S values or $\Delta_A = |D|(S^2 - 1/4)$ for half-integer S values (according to the Hamiltonian $H = DS_z^2$, where S_z is a component of S in the z direction).[7] In addition to this anisotropic barrier, however, SCMs experience an additional component to the overall relaxation barrier stemming from short-range magnetic correlation along the molecular chain, which is described by the correlation energy barrier Δ_ξ. Therefore, in this finite-size region, the total energy needed to invert the magnetization is $\Delta_\tau = \Delta_\xi + \Delta_A$,[8] where Δ_A is the anisotropic energy barrier of one domain wall.

For one-dimensional systems falling within the Ising limit, the correlation energy is related to the intrachain coupling strength J and constituent spins through the equation $\Delta_\xi = 4|JS_1S_2|$. Recently, Long and co-workers reported a series of $(DMF)_4MRe^{IV}Cl_4(CN)_2$ (DMF = dimethylformamide; M = Mn^{II}, Fe^{II}, Co^{II}, and Ni^{II}) SCMs[3] in which the correlation energy Δ_ξ was far smaller than $4|JS_1S_2|$. They did not fall within the Ising limit with sharp domain walls because the anisotropic energy was not sufficiently larger than the exchange energy. Until now, however, there has been no clear expression of Δ_ξ in terms of J and S in the intermediate region between the Ising and Heisenberg limits.

To explore the origin of the energy barriers and the expressions of Δ_ξ and Δ_A in terms of D, J, and S for SCMs in the intermediate region between the Ising and Heisenberg limits, we used density functional theory (DFT), complete active space self-consistent field (CASSCF), and complete active space second-order perturbation theory (CASPT2), considering the effect of the dynamical electronic correlation based on CASSCF methods, to investigate the magneto-structural correlations in a family of $R_4Fe^{II}Re^{IV}Cl_4(CN)_2$ SCMs, where R = diethylformamide (DEF) (**1**), dibutylformamide (DBF) (**2**), DMF (**3**), dimethylbutyramide (DMB) (**4**), dimethylpropionamide (DMP) (**5**), and diethylacetamide (DEA) (**6**).[4] Considering the similar structures of complexes **1**–**6**, only the structure of complex **3** is shown in Figure 1. A detailed description of these structures can be found in references 3 and 4.

Received: November 27, 2013
Published: March 27, 2014

   dx.doi.org/10.1021/ic402945j | Inorg. Chem. 2014, 53, 3503−3510

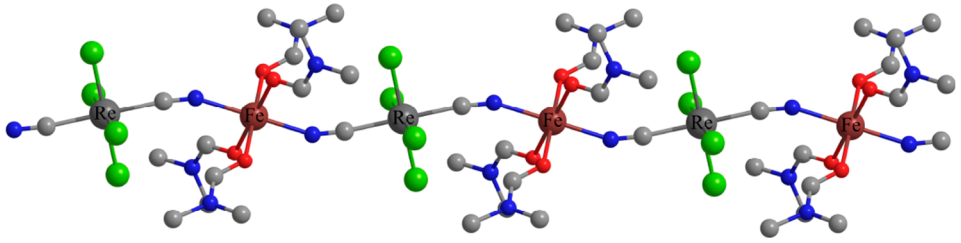

Figure 1. Structure of $(DMF)_4Fe^{II}Re^{IV}Cl_4(CN)_2$ (**3**); H atoms are neglected for clarity.

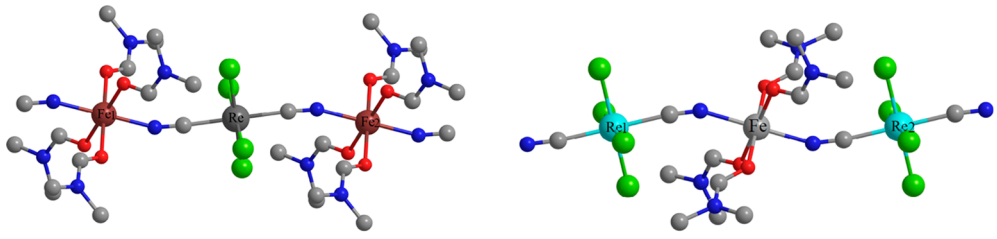

(*a*) (*b*)

Figure 2. Structure of models **A** $(DMF)_4Fe^{II}[Re^{IV}Cl_4(CN)_2]_2$ (a) and **B** $[(DMF)_4Fe^{II}CN]_2Re^{IV}Cl_4(CN)_2$ (b); H atoms are neglected for clarity.

1. COMPUTATIONAL DETAILS

The spin Hamiltonian for an alternating classical-spin Heisenberg chain is expressed as:

$$H = -2J \sum_{i}^{\infty} (S_{Rei}S_{Fei} + S_{Rei}S_{Fei+1}) \quad (1)$$

where J represents the exchange coupling constant for the interaction between neighboring Re^{IV} and Fe^{II} centers, and S_{Re} and S_{Fe} are the local spins of Re^{IV} ($S = 3/2$) and Fe^{II} ($S = 2$), respectively. Long and co-workers demonstrated that the use of an isotropic Heisenberg model to describe the exchange couplings of $R_4Fe^{II}Re^{IV}Cl_4(CN)_2$ was appropriate, irrespective of the highly anisotropic $[ReCl_4(CN)_2]^{2-}$ unit inside the chain.[3,4]

To obtain the isotropic exchange coupling constant J, Orca 2.9.1 calculations[9] were performed with the popular B3LYP hybrid functional proposed by Becke[10,11] and Lee et al.[12] Triple-ζ with one polarization function TZVP[13] basis set was used for all atoms. The scalar relativistic treatment (ZORA) was used in all calculations. The large integration grid (grid = 5) was applied to Re and Fe for ZORA calculations. Tight convergence criteria were selected to ensure that the results were well converged with respect to technical parameters. We employed two model structures of **A** and **B** (see Figure 2a,b) for each complex and calculated two high-spin and one low-spin state energy for each model: $S_{HS} = S_{Fe1} + S_{Re} + S_{Fe2}$ for model **A**; $S_{HS} = S_{Re1} + S_{Fe} + S_{Re2}$ for model **B**, $S_{LS} = S_{Fe1} - S_{Re} + S_{Fe2}$ with the flipped spins of Re^{IV} for model **A**; $S_{LS} = S_{Re1} - S_{Fe} + S_{Re2}$ with the flipped spins of Fe^{II} for model **B**. The Re^{IV}–Fe^{II} coupling constant J was then obtained as eq 2 according to the spin Hamiltonian $H = -2JS_{Re}(S_{Fe1} + S_{Fe2})$ for model **A** and $H = -2JS_{Fe}(S_{Re1} + S_{Re2})$ for model **B**.

$$J = \frac{E_{LS} - E_{HS}}{30} \quad (2)$$

To obtain D, Orca 2.9.1 calculations[9] were performed with the generalized gradient approximation (GGA) Perdew, Burke, and Ernzerhof (PBE)[14] functional, which has been tested by Neese and other authors.[15] Other GGA functionals will yield very similar results and were not repeated here. The spin–orbit coupling (SOC) was treated effectively using the multicenter spin–orbit mean-field (SOMF) method developed by Hess et al.[16] The coupled-perturbed (CP) method proposed by Neese was used,[15] which uses revised prefactors for the spin-flip terms and solves a set of CP equations for the SOC perturbation. The triple-ζ with one polarization function TZVP[13] basis sets for all atoms were used in all calculations. Tight convergence criteria were used to ensure that the results were well-converged with respect to technical parameters. The D and E values were obtained in their spin ground states.

DFT is usually a poor method to calculate the D value of those highly anisotropic magnetic ions.[17] More accurate methods, such as CASSCF and CASPT2, were used to evaluate the D values of Re^{IV} in $Re^{IV}Cl_4(CN)_2Zn_2$ and of Fe^{II} in $Fe^{II}R(CN)_2Ba_2$ fragments with the MOLCAS 7.8 program package.[18] To calculate the D value of the Re^{IV} fragment (see Figure 3a), the influence of the neighboring Fe^{II} ions was taken into account using the closed-shell Zn^{II} ab initio embedding model potentials (AIMP; Zn.ECP.Lopez-Moraza.0s.0s.0e-AIMP-$KZnF_3$.).[19] The only removed atoms were those connected to Zn^{II} AIMP from the opposite side of the molecule. Similarly, the neighboring Re^{IV} ions were simulated using the closed-shell Ba^{II} AIMP (Ba.ECP.Pascual.0s.0s.0e-AIMP-BaF_2.)[19] to calculate the D value of the Fe^{II} fragment (Figure 3b).

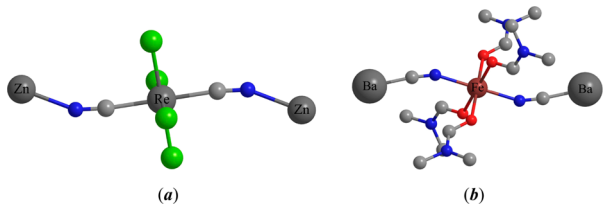

(*a*) (*b*)

Figure 3. Calculated Re^{IV} ($Re^{IV}Cl_4(CN)_2Zn_2$) (a) and Fe^{II} ($Fe^{II}R(CN)_2Ba_2$) (b) fragments; H atoms are neglected for clarity.

For CASSCF calculations, the basis sets for all atoms were the atomic natural orbitals from the MOLCAS ANO-RCC library: ANO-RCC-VTZP for Re^{IV} and Fe^{II} ions, VTZ for nearby Cl, O, C, and N atoms, and VDZ for distant atoms.

dx.doi.org/10.1021/ic402945j | Inorg. Chem. 2014, 53, 3503–3510

Table 1. Experimental Fe−N−C and Re−C−N Angles and the Calculated and Experimental J Values (cm^{-1}) of Six $R_4Fe^{II}Re^{IV}Cl_4(CN)_2$ Compounds[a]

	1		2		3		4		5		6	
	A	B	A	B	A	B	A	B	A	B	A	B
∠Fe−N−C	154.7		157.6		158.0		164.4		170.6		180.0	
∠Re−C−N	173.3		173.2		175.3		179.7		176.6		180.0	
J cal.	5.1	4.8	5.0	4.9	5.8	5.4	6.0	5.7	5.5	5.3	8.1	5.7
exp.[4]	4.2(2)		4.5(2)		4.8(4)		5.6(3)		6.3(2)		7.2(3)	

[a]R = DEF (**1**), DBF (**2**), DMF (**3**), DMB (**4**), DMP (**5**), DEA (**6**).

ANO-RCC-VTZ basis sets were also used for the distant N atoms in $Re^{IV}Cl_4(CN)_2$ fragment calculations. The SOC effect was calculated by the restricted active space interaction (RASSI-SO) procedure. The active space was (3, 5) and (6, 5) for Re^{IV} and Fe^{II}, respectively. We mixed all spin-free states (Re, 40; Fe, 100) in each fragment calculation.

For fragments including more than one magnetic center, we did not calculate the total D using CASSCF and CASPT2 for the large computational demand, due to the large active space and number of atoms. Rather, we calculated the D value of the large fragment projecting the single-site anisotropies (D_i) onto the spin ground state S.

$$D = \sum_{i=1}^{N} d_i D_i \tag{3}$$

where i numbers the N metal centers and the d_i values were projection coefficients. Equation 3 was derived in the strong-exchange limit for a spin cluster. The anisotropic interaction tensor D_{ij} was ignored, since dipolar and anisotropic interactions yielded only minor contributions, especially for our studied cyanide-bridged complexes where the metal−metal distances were large.

2. RESULTS AND DISCUSSION

Evaluation and Comparison of the Exchange Interactions. The DFT calculated and experimental J values of six $R_4Fe^{II}Re^{IV}Cl_4(CN)_2$ compounds are shown in Table 1. The positive J values of compounds **1**−**6** indicate that all the Re^{IV}−Fe^{II} couplings were ferromagnetic.

To probe the mechanism of the Re^{IV}−Fe^{II} exchange couplings, we evaluated three magnetic orbitals localized on one Re^{IV} (t_{2g}^3) and four on the neighboring Fe^{II} ($t_{2g}^4e_g^2$) of compound **6** (Figure 4). There were two magnetic exchange pathways through cyanide between $Re^{IV}(t_{2g}^3)$ and $Fe^{II}(t_{2g}^2e_g^2)$. First, two π−π interactions occurred in $Re^{IV}(t_{2g}^3)$ orbitals (left in Figure 4) through cyanide π^* orbitals with the $Fe^{II}(t_{2g}^2)$ orbitals (the d_{xy} and d_{yz} orbitals on the right in Figure 4), resulting in antiferromagnetic coupling. Second, two σ−π interactions between electrons in orthogonal $Fe^{II}(e_g^2)$ (the d_{z^2} and $d_{x^2-y^2}$ orbitals on the right in Figure 4) and $Re^{IV}(t_{2g}^3)$ orbitals, respectively, should give rise to ferromagnetic exchange. Two kinds of competitive interactions often lead to net ferromagnetic coupling, since σ-type interactions are invariably stronger than π-type interactions.[4]

The Re^{IV}−Fe^{II} ferromagnetic couplings strengthened as the Fe−N−C angle increased (experimental J values, Table 1). The Re−C−N angle had little influence on the Re^{IV}−Fe^{II} couplings, as noted by the small difference between the J values of complexes **2** and **3**. Their Fe−N−C angles were almost the same. Although the trend of the calculated J values of the six SCMs was not completely identical to the experimental one, the obtained J values using models **A** and **B** were very close to the experimental ones. Compound **6** had two different Re^{IV}−Fe^{II} couplings, leading to larger differences in the J values found in models **A** and **B**. In the next section, we investigate it thoroughly. The small difference in the structures except for the Fe−N−C and Re−C−N angles may slightly influence the final calculated J values due to the systematic error in the DFT calculations. To thoroughly investigate the relationship between the J value and the Fe−N−C angle, we selected compound **4** as an example, as its calculated and experimental J values were very close. We calculated the J values using model **A** with Fe−N−C angle from 140° to 180°. The corresponding J, spin population of Re^{IV}, and spin population of Fe^{II} are shown in Table 2. The spin population on Re^{IV} and Fe^{II} was obtained using Mulliken Population Analysis,[20] calculated with the B3LYP functional. The spin populations of two Fe^{II} ions were the same because of symmetry. Both the J values and the spin populations of Re^{IV} and Fe^{II} increased as the Fe−N−C angle increased (Table 2).

According to Kahn's theory,[21] the exchange coupling constant J_{ab} is expressed as:

$$J_{ab} \approx K_{ab} - S_{ab}(\Delta^2 - \delta^2)^{1/2} \tag{4}$$

The positive term, K_{ab}, represented the ferromagnetic contribution J_F, favoring parallel alignment of the spins, while the negative term $-S_{ab}(\Delta^2-\delta^2)^{1/2}$ was the antiferromagnetic contribution J_{AF}, favoring antiparallel alignment of the spins. S_{ab} was the overlap integral between the magnetic orbitals a and b. δ was the initial energy gap between magnetic orbitals, and Δ was the energy gap between the molecular orbitals derived from them. When several electrons were present on each center, n_i on one side and n_j on the other, J was described by the sum of the different "orbital pathways" J_{ab}, defined as for the pairs of orbitals a and b located on each site, and weighted by the number of electrons in eq 5.

$$J = \Sigma_{a,b} J_{ab}/n_i \times n_j \tag{5}$$

There are several different contributions to the exchange coupling constant in each Re^{IV}−Fe^{II} pair. According to eq 6, proposed by Ruiz and co-workers,[22] the square of the mean overlap integral S_{ij} between magnetic orbitals on the paramagnetic centers i and j can be correlated to the Δ_{ij} for polynuclear complexes.

$$\Delta_{ij} = \left(\sqrt{|(\rho^i_{HS})^2 - (\rho^i_{LS})^2|} + \sqrt{|(\rho^j_{HS})^2 - (\rho^j_{LS})^2|}\right)^2 \tag{6}$$

where ρ^i_{HS}, ρ^i_{LS}, ρ^j_{HS}, and ρ^j_{LS} are the spin populations of the centers i and j involved in the exchange interaction of the high- or low-spin configurations, respectively.

The changes in the J_{AF} term are more important, and these contributions usually dominate the magneto-structural correlations.[23] Hence, variation of J was correlated with the changes in

dx.doi.org/10.1021/ic402945j | Inorg. Chem. 2014, 53, 3503−3510

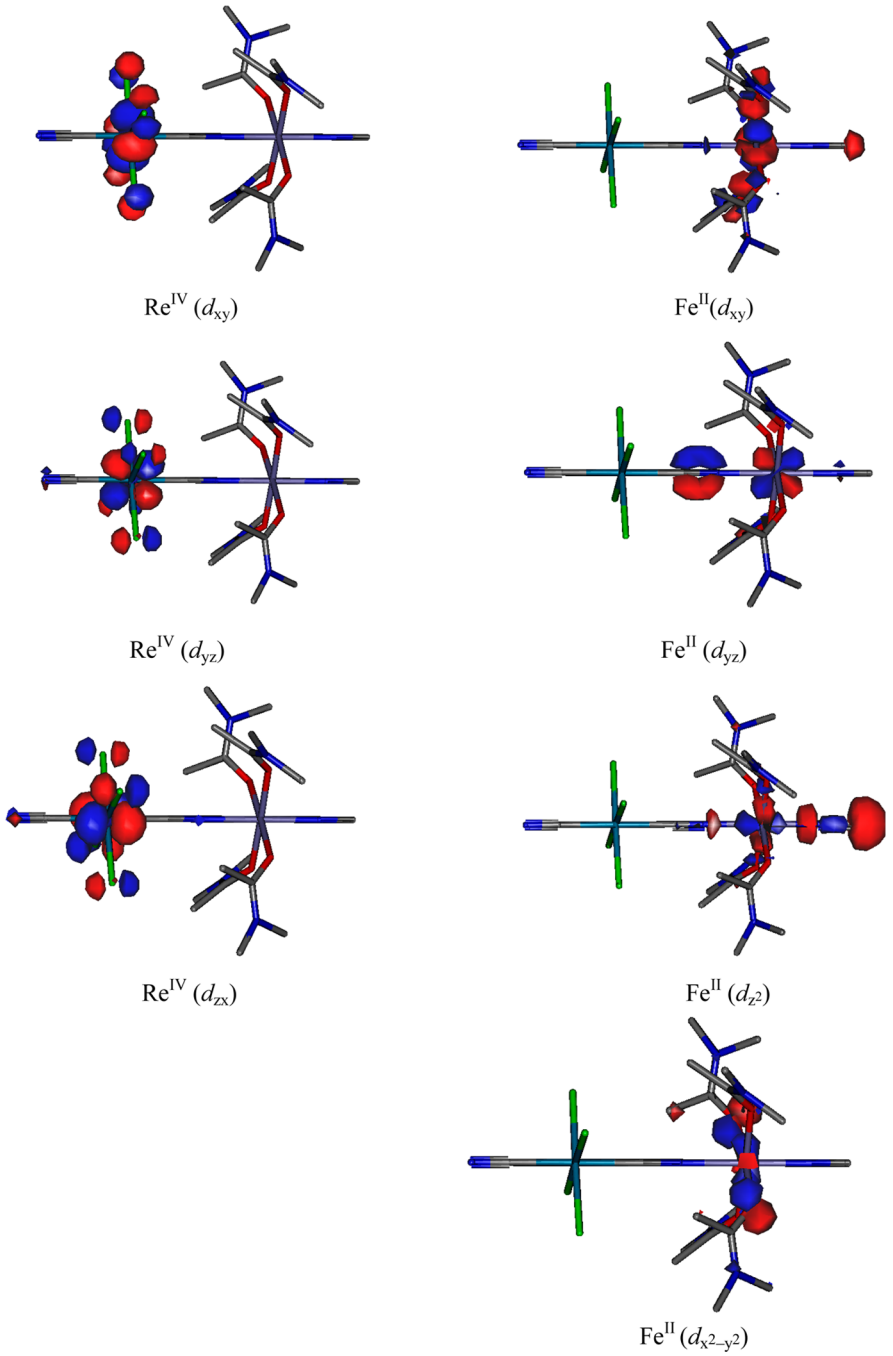

Figure 4. Magnetic orbitals of one Re^{IV} (left) and of the neighboring Fe^{II} (right) of compound **6** in the low-spin state.

Table 2. Calculated *J* Values (cm^{-1}) and the Spin Density Populations (e) of Re^{IV} and Fe^{II} in the High- and Low-Spin States of Compound 4 Using Model A with the Fe−N−C Angle Ranging from 140° to 180°

∠Fe−N−C, deg	140	145	150	155	160	164.4	170	175	180
Re^{IV}	2.331	2.398	2.424	2.434	2.441	2.446	2.451	2.465	2.476
	−2.337	−2.401	−2.423	−2.433	−2.440	−2.445	−2.449	−2.464	−2.475
Fe^{II}	3.838	3.842	3.844	3.846	3.847	3.848	3.850	3.852	3.854
	3.822	3.825	3.829	3.832	3.836	3.839	3.843	3.847	3.851
J^a	2.1	2.9	4.0	5.0	5.7	6.0	6.5	7.2	8.3

[a]Kahn's qualitative theory[21] was used to interpret these magneto-structural correlations.

the J_{AF} term according to the equation $J = J_F + J_{AF}$. The strength of J_{AF} is linearly dependent on Δ_{ij}.[22]

$$|J_{AF}| \propto S_{ij}^2 \propto \Delta_{ij} \quad (7)$$

The relationship between Δ_{ij} and the Fe−N−C angle of compound **4**, ranging from 140° to 180°, is shown in Figure 5. The Δ_{ij} values decreased as the Fe−N−C angle increased. The decrease of Δ_{ij} led to a decrease of the absolute value of S_{ij} and

dx.doi.org/10.1021/ic402945j | Inorg. Chem. 2014, 53, 3503−3510

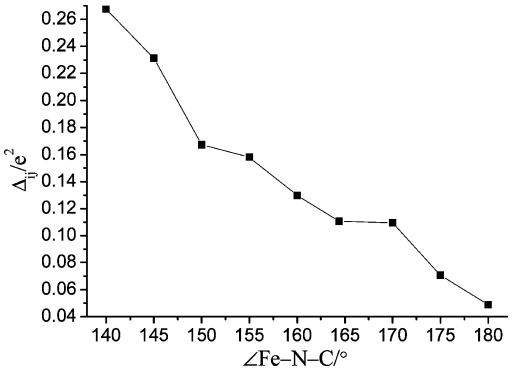

Figure 5. Dependence of Δ_{ij} on Fe−N−C angle of compound **4** (140° to 180°).

a decrease of the J_{AF} term. Thus, the positive Re^{IV}−Fe^{II} coupling constants J ($J = J_F + J_{AF}$) increased as the Fe−N−C angle increased from 140° to 180°, in accordance with the experimental trend.

Evaluation of Methods Used to Investigate the Magnetic Anisotropy. The above results show that B3LYP can predict J values used in the calculation of Re^{IV}−Fe^{II} coupling constants. Does it also work well in the calculation of the magnetic anisotropic parameters D and E of **1**−**6**? To answer this question, we selected the following four SMMs, which were associated with our investigated SCMs: $[Re^{IV}Cl_4(CN)_2]^{2-}$,[3,6] $(DMF)_4ZnReCl_4(CN)_2$,[6] $[TPA^{2C(O)NHtBu}Fe^{II}(CF_3SO_3)]^{+}$[24], and $(TPA^{2C(O)NHtBu})Fe^{II}Re^{IV}Cl_4(CN)_2$.[25] These had structural similarity to the SCMs we previously evaluated. We calculated their D values using the DFT method, with PBE functional, and the ab initio methods of CASSCF and CASPT2. Since B3LYP cannot give a more accurate D value, only PBE was used in the calculation.[15] The calculated and experimental D and E values of the four SMMs are shown in Table 3. CASPT2 was found to give more accurate values of D for the first two SMMs, very close to the experimental ones, while PBE and CASSCF were less satisfactory in this regard.

The D values of $[Re^{IV}Cl_4(CN)_2]^{2-}$ and $(DMF)_4ZnReCl_4(CN)_2$ predicted by PBE and CASSCF methods were far from the experimental values, sometimes even having the opposite sign. The PBE and CASSCF methods also produced poor D values of $[TPA^{2C(O)NHtBu}Fe^{II}(CF_3SO_3)]^{+}$. The CASPT2 method provided the most accurate D values. The E values of $[Re^{IV}Cl_4(CN)_2]^{2-}$, $(DMF)_4ZnReCl_4(CN)_2$, and $[TPA^{2C(O)NHtBu}Fe^{II}(CF_3SO_3)]^{+}$ obtained by using CASPT2 were closest to the experimental values.

The total D value of $(TPA^{2C(O)NHtBu})Fe^{II}Re^{IV}Cl_4(CN)_2$ was also predicted using CASSCF and CASPT2 methods from the calculated local D_i values of the $Re^{IV}Cl_4(CN)_2Zn$ and $(TPA^{2C(O)NHtBu})Fe^{II}Ba$ fragments (see Figure 3), according to eq 3. The hard and easy axes of $Re^{IV}Cl_4(CN)_2Zn$ and $(TPA^{2C(O)NHtBu})Fe^{II}Ba$ fragments were calculated using CASPT2 (Figure 6).

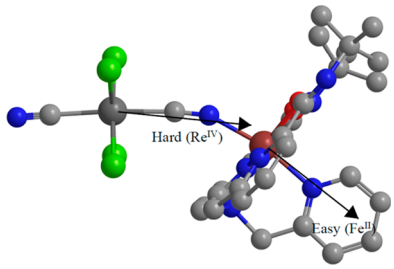

Figure 6. Alignment of the local hard and easy axes of $Re^{IV}Cl_4(CN)_2Zn$ and $(TPA^{2C(O)NHtBu})Fe^{II}Ba$ fragments.

The D_i and E_i values of the $Re^{IV}Cl_4(CN)_2Zn$ fragment extracted from $(TPA^{2C(O)NHtBu})Fe^{II}Re^{IV}Cl_4(CN)_2$ were calculated using CASPT2 and were found to be 15.7 and 4.8 cm^{-1}, respectively. The D_i and E_i values of the $(TPA^{2C(O)NHtBu})Fe^{II}Ba$ fragment were found to be −5.8 and −1.07 cm^{-1}, respectively. The $Re^{IV}Cl_4(CN)_2Zn$ fragment had doubly degenerate $M_S = \pm 1/2$ ground levels related to an isolated $S = 3/2$ molecule with a positive D value. This prevented localization of the molecular magnetic moment within the xy plane due to the quantum tunneling effect. Thus, the total D value of $(TPA^{2C(O)NHtBu})Fe^{II}Re^{IV}Cl_4(CN)_2$ was mainly due to the contribution of the $(TPA^{2C(O)NHtBu})Fe^{II}Ba$ fragment. According to eq 3, the D value of $(TPA^{2C(O)NHtBu})Fe^{II}Re^{IV}Cl_4(CN)_2$ predicted by CASPT2 was −1.7 cm^{-1} ($D = 6/21 \times (-5.8)$), closest to the experimental value, while CASSCF gave the much larger D value using the above approach.

In conclusion, the PBE and CASSCF methods were poor in predicting the values of D and E in our studied systems. In the following section, CASPT2 was used to express Δ_ξ and Δ_A in terms of D, J, and S, and the origin of the magnetic anisotropy energy barriers for six $Fe^{II}Re^{IV}(CN)_2$ SCMs.

Origin of the Magnetic Anisotropic Energy Barrier. As usual, for one-dimensional systems falling within the Ising limit, Δ_ξ can be expressed as $4|JS_1S_2|$. In the case of compound **3**, however, the experimental Δ_ξ value was 28 cm^{-1},[3] far smaller than the predicted $4JS_{Re}S_{Fe}$ value (57.6 cm^{-1}). The experimental Δ_ξ values of the SCMs are rarely reported.[4] However, the total energy barriers Δ_τ of compounds **1**−**5** have been shown to be smaller than $4JS_{Re}S_{Fe}$. Compounds **1**−**5** did not fall within the Ising limit. Compound **6** had a higher $4JS_{Re}S_{Fe}$ value of 86.4 cm^{-1}, close to the total energy barrier Δ_τ of 93 cm^{-1}.[4] In fact, the following calculation results show that **6** does not fall within the Ising limit either.

To explore the constitution of the domain walls and the expressions of Δ_ξ and Δ_A using D, J, and S, we first calculated the D_i and E_i values of the Re^{IV} ($Re^{IV}Cl_4(CN)_2Zn_2$) and Fe^{II} ($Fe^{II}R(CN)_2Ba_2$) fragments extracted from the six SCMs, respectively (Table 4).

Homospin chains with collinear anisotropy axes that have a D_i/J ratio greater than 4/3 have sharp domain walls with a creation energy predicted by $\Delta_\xi = 4|J|S_1S_2$.[8] For our investigated heterospin $Fe^{II}Re^{IV}(CN)_2$ SCMs, we assumed the anisotropy axes were parallel and concluded that, when the D_i/J ratio was

Table 3. Calculated and Experimental $D(E)$ Values (cm^{-1}) of Four SMMs

SMM	$[Re^{IV}Cl_4(CN)_2]^{2-}$	$(DMF)_4ZnReCl_4(CN)_2$	$[TPA^{2C(O)NHtBu}Fe^{II}(CF_3SO_3)]^{+}$	$(TPA^{2C(O)NHtBu})Fe^{II}Re^{IV}Cl_4(CN)_2$
PBE	−29.5 (0.03)	−33.7(0.06)	−2.1 (−0.49)	−8.5 (−2.60)
CASSCF	−23.1(1.75)	−21.5(1.78)	−30.2 (−0.36)	−5.6
CASPT2	13.1(2.6)	11.2(2.5)	−6.7 (−1.02)	−1.7
exp.	11.1(3.2)[6]	11.0 (2.1)[6]	−7.9 (−2.01)[24]	−2.3[25]

dx.doi.org/10.1021/ic402945j | Inorg. Chem. 2014, 53, 3503−3510

Table 4. Calculated D_i, E_i, $(D_i - E_i)/J$, and $2|E_i|/J$ Values (cm^{-1}) of Fe^{II} ($Fe^{II}R(CN)_2Ba_2$) and Re^{IV} ($Re^{IV}Cl_4(CN)_2Zn_2$) Fragments Where J Was the Experimental Re^{IV}–Fe^{II} Coupling Constant (cm^{-1}) of Six SCMs

	1		2		3		4		5		6	
	Re^{IV}	Fe^{II}	Re^{IV}	Fe^{II}	Re^{IV}	Fe^{II}	Re^{IV}	Fe^{II}	Re^{IV}	Fe^{II}	Re^{IV}	Fe^{II}
D_i	5.8	−7.5	10.3	−8.7	11.4	−9.2	20.8	−7.6	19.8	−7.5	5.9	−7.6
E_i	2.86	−1.65	1.07	−1.47	3.38	−1.63	1.59	−2.01	3.26	−1.79	1.15	−1.34
$(D_i - E_i)/J$		1.39		1.61		1.57		0.99		0.91		0.87
$2\|E_i\|/J$	1.36		0.48		1.41		0.57		1.03		0.32	
J	4.2		4.5		4.8		5.6		6.3		7.2	

larger than 2 for Re^{IV} and 1 for Fe^{II}, sharp domain walls were present, according to Barbara and co-workers' theory, where $\Delta_A > 1/3\Delta_\xi$.[26] Since the rhombic anisotropy of Fe^{II} will shortcut the energy barrier, we replaced D_i using $D_i - E_i$ and defined the ratio as $(D_i - E_i)/J$. Long and co-workers reported that for an easy-plane system, the anisotropy energy associated with the reversal of a single Re^{IV} spin within a chain was given by $\Delta_A = 2|E|S^2$, where $E = (D_x - D_y)/2$.[6] Thus, for the Re^{IV} fragments with positive D values, we substituted $(D_i - E_i)/J$ using $2|E_i|/J$ to define the ratio. The $2|E_i|/J$ values of Re^{IV} of compounds **1**–**6** were all less than 2; the $(D_i - E_i)/J$ values of Fe^{II} of compounds **1**–**3** were all greater than 1, while those of **4**–**6** were less than 1(Table 4).

We separated six SCMs into two groups based on their $2|E_i|/J$ and $(D_i - E_i)/J$ values of Re^{IV} and Fe^{II} in Table 4. The first group compounds **1**–**3** had $2|E_i|/J$ values of Re^{IV} less than 2, while the $(D_i - E_i)/J$ values of Fe^{II} were greater than 1. In contrast, the $(D_i - E_i)/J$ values of Fe^{II} of compounds **4**–**6** (the second group) were less than 1. Since the magnetic anisotropic energies of Fe^{II} fragments for compounds **1**–**6** were all far greater than the rhombic anisotropy energies of Re^{IV} fragments, the spins on Re^{IV} were orientated in the directions of the spins on Fe^{II}. This was due to the strong Re^{IV}–Fe^{II} ferromagnetic interactions (Table 4). In Figure 7, we show the easy plane

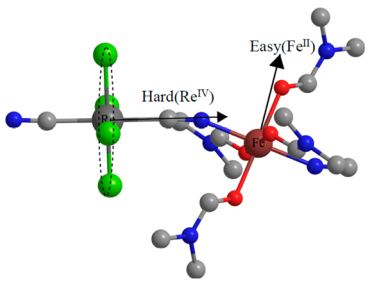

Figure 7. Alignment of the local easy plane and axis of Re^{IV} ($Re^{IV}Cl_4(CN)_2Zn_2$) and Fe^{II} ($Fe^{II}R(CN)_2Ba_2$) fragments of compound **3**, respectively.

and axis on the Re^{IV} and Fe^{II} fragments of compound **3**. The easy planes and axes of Re^{IV} and Fe^{II} fragments of the other complexes were very similar to those of compound **3**.

The easy axes of Fe^{II} were all strictly parallel in the six $Fe^{II}Re^{IV}(CN)_2$ SCMs. Figure 7 shows that the easy axis of Fe^{II} did not lie in the easy plane of Re^{IV} in compound **3**. The inclined angles between the easy axes of Fe^{II} and the hard axes of Re^{IV} for compounds **1**–**5** were 56.4°, 59.2°, 63.6°, 71.4°, and 80.1°, respectively. In compound **6**, however, the easy axis of Fe^{II} was almost parallel to the easy plane of Re^{IV}. Because of the much smaller rhombic anisotropy energy of Re^{IV} compared to the energy barrier of Fe^{II} (Table 4), the spins of Re^{IV} were orientated in the direction of the spins of Fe^{II} under the strong Re^{IV}–Fe^{II} ferromagnetic coupling interactions. Thus, although the easy planes on Re^{IV} and the easy axes of Fe^{II} were not parallel, the $(D_i - E_i)/J$ and $2|E_i|/J$ values could be used as a reference since the total energy barrier mainly came from the contribution of Fe^{II}, whose easy axes were strictly parallel.

According to the above analysis, each unit cell of $Fe^{II}R$ in compounds **1**–**3** could be regarded as a domain wall since the $(D_i–E_i)/J$ values of Fe^{II} were all greater than 1. The total energy barrier Δ_τ of compounds **1**–**3** were closely equal to the creation energy of flipping the spins on one Fe^{II}. This corresponded to the amount of energy needed to overcome the magnetic anisotropy energy Δ_A, $(D_i–E_i)S_{Fe}^2$, and the correlation energy Δ_ξ mainly coming from the exchange interaction between Fe^{II} and the neighboring Re^{IV}. When the spins of one Fe^{II} flipped, the spins of the neighboring Re^{IV} simultaneously flipped due to the small rhombic anisotropy energy of Re^{IV}. But the spins were not in the same direction of the spins of Fe^{II} due to the exchange interaction of Fe^{II} on the other side. When the spin of one Fe^{II} completely flipped to the opposite direction, the spins of the central Re^{IV} were orientated to a direction perpendicular to it due to the competing interactions of the two neighboring Fe^{II} located in the adjacent Re^{IV} (Figure 8). Thus, the correlation

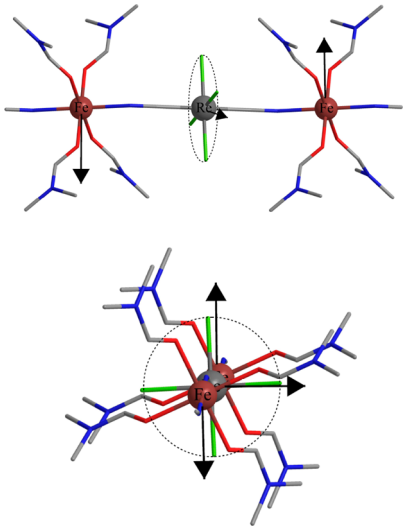

Figure 8. Alignment of the spins of one Fe^{II} (left or front), the central Re^{IV}, and the other Fe^{II} (right or behind) when the spins of the left or front Fe^{II} completely flipped to the opposite direction.

energy barriers Δ_ξ of compounds **1**–**3** were all closely equal to half of $4JS_{Re}S_{Fe}$ (Table 5).

The calculated total energy barriers $\Delta_\tau = \Delta_A + \Delta_\xi$ are close to the experimental values for those of compounds **1**–**3**, respectively, and the variation trend of the Δ_τ from **1** to **3** is the same with the experimental one.

dx.doi.org/10.1021/ic402945j | Inorg. Chem. 2014, 53, 3503–3510

Table 5. Calculated and Experimental Δ_A, Δ_ξ, and Δ_τ Values of Compounds 1−3 (cm^{-1})

	Δ_A		Δ_ξ		Δ_τ	
	cal.	exp.	cal.	exp.	cal.	exp.[4]
1	23.4		25.2		48.6	45.0
2	28.9		27.0		55.9	55.0
3	30.3	28.0	28.8	28.0	58.3	56.0

For compounds **4** and **5** (the second group), since the $(D_i - E_i)/J$ of Fe^{II} were less than 1, each domain wall contained more than one unit cell of $Fe^{II}R$. When the spins of one Fe^{II} flipped, the spins of the neighboring Re^{IV} also simultaneously flipped, following them. The third neighboring Fe^{II} also flipped due to its small $(D_i - E_i)/J$ value. When the spin of one Fe^{II} completely flipped, the direction of the spin of the Fe^{II} ion, the central Re^{IV}, and the other neighboring Fe^{II} were not perpendicular to each other (Figure 9).

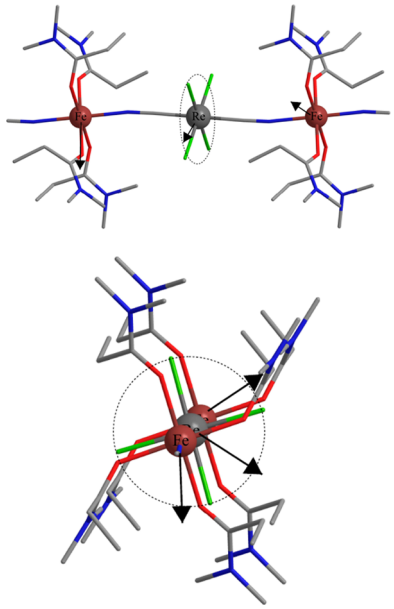

Figure 9. Alignment of the spin of one Fe^{II} (left or front), the central Re^{IV}, and the other Fe^{II} (right or behind) when the spins on the left or front Fe^{II} completely flipped to the opposite direction.

For compound **4** or **5**, although the calculated anisotropy energy barrier of Fe^{II} was also larger than one-third of $2JS_{Re}S_{Fe}$ ($\Delta_A > 2/3JS_{Re}S_{Fe}$), the energy barrier from $S_z = 2$ to $S_z = 1$ was smaller than one-third of $2JS_{Re}S_{Fe}$. Therefore, the other neighboring Fe^{II} spin $S = 2$ was orientated to $S_z = 1$ (the projection of the Fe^{II} spin $S = 2$ on its easy axis). The total energy barrier Δ_τ of compounds **4** and **5** was closely equal to the creation energy required to flip the spin of one Fe^{II}. This energy requirement would need to overcome the anisotropic energy barrier Δ_A, $(D_i - E_i){S_{Fe}}^2$, and the correlation energy barrier Δ_ξ coming from the exchange interaction on the left Fe^{II} from the central Re^{IV}, which is about $2JS_{Re}S_{Fe}(\cos 98.4 - \cos 180)$. The inclined angle between the spins of the left Fe^{II} and the central Re^{IV} were close to 81.6° due to the competing exchange interactions of the two neighboring Fe^{II}. The calculated and experimental Δ_A, Δ_ξ, and Δ_τ values are shown in Table 6.

The values of Δ_τ obtained from the calculated Δ_A and Δ_ξ of compounds **4** and **5** were a little larger than the corresponding experimental values because the orientation of the spins on the

Table 6. Calculated and Experimental Δ_A, Δ_ξ, and Δ_τ Values (cm^{-1}) of Compounds 4 and 5

	Δ_A	Δ_ξ	Δ_τ	
	cal.	cal.	cal.	exp.[4]
4	22.4	28.7	51.1	49
5	22.8	32.3	55.1	53

right or behind Fe^{II} (Figure 9) in the $S_z = 1$ state was difficult to be accurately defined (Table 6).

It was evident that compound **6** did not fall into the Ising limit with sharp domain walls. It was not clear why its total energy barrier Δ_τ was the highest to 93 cm^{-1}. The structure of compound **6** (Figure 10) contained two different Re^{IV}−Fe^{II}

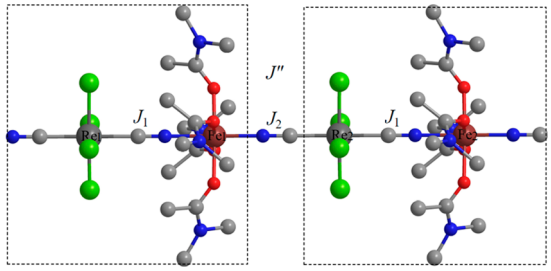

Figure 10. Structure of compound **6**; H atoms are omitted for clarity.

exchange coupling constants, J_1 and J_2, compared to only one in compounds **1**−**5**.

It was assumed that the two exchange coupling constants of J_1 and J_2 of compound **6** were the same in both the above calculation and the experimental fitting. To obtain the different J_1 and J_2 values, we calculated the energies of three spin states (see Figure 2a): the high-spin state ($S_{HS} = S_{Fe1} + S_{Re} + S_{Fe2}$), the first low-spin state (flip the spins of Fe1; $S_{LS1} = -S_{Fe1} + S_{Re} + S_{Fe2}$), and the second low-spin state (flip the spins of Fe2; $S_{LS2} = S_{Fe1} + S_{Re} - S_{Fe2}$). The calculated J_1 and J_2 values were 9.6 cm^{-1} and 5.5 cm^{-1}, respectively, according to eqs 8 and 9.

$$J_1 = (E_{LS1} - E_{HS})/15 \quad (8)$$

$$J_2 = (E_{LS2} - E_{HS})/15 \quad (9)$$

The values of $2|E_i|/J_1$ and $2|E_i|/J_2$ for Re^{IV} were both less than 2. However, the value of $(D_i - E_i)/J_1$ for Fe^{II} was less than 1, while the $(D_i - E_i)/J_2$ value was greater than 1. Thus, we can approximate one Re1Fe1 or Re2Fe2 (Figure 10) as a unit cell (one domain wall). The exchange coupling constant J'' between the neighboring unit cells of Re1Fe1 and Re2Fe2 are described by the spin Hamiltonian: $H = -2J_1(S_{Re1}S_{Fe1} + S_{Re2}S_{Fe2}) - 2J_2S_{Re1}S_{Fe2}$ and $H = -2J''S_{Re1Fe1}S_{Re2Fe2}$.

$$J'' = \frac{15}{56}J_2 \quad (10)$$

The $\Delta_\xi = 4J''S_{Re1Fe1}S_{Re2Fe2}$ of compound **6** was 72.2 cm^{-1} (eq 10). To obtain Δ_A, we first calculated the total D_{Re1Fe1} value of one unit cell of Re1Fe1 (eq 3). Because of the positive D and the small E values of Re^{IV} of compound **6**, the total D_{Re1Fe1} value mainly originated from the contribution of the Fe1. The obtained D_{Re1Fe1} and E_{Re1Fe1} ($D_{Re1Fe1} = 6/21D_{Fe1}$; $E_{Re1Fe1} = 6/21E_{Fe1}$) values were −2.2 cm^{-1} and −0.38 cm^{-1}, respectively. The anisotropic energy barrier $\Delta_A = [(D_{Re1Fe1} - E_{Re1Fe1})\text{-}({S^2}_{Re1Fe1} - 1/4)]$ was then calculated as 21.8 cm^{-1}. Using the above calculated Δ_ξ and Δ_A, the total energy barrier Δ_τ of

dx.doi.org/10.1021/ic402945j | Inorg. Chem. 2014, 53, 3503−3510

compound **6** was 94.0 cm^{-1}, very close to the experimental value of 93 cm^{-1}.[4]

The above analysis shows that the total energy barriers for the six $Fe^{II}Re^{IV}(CN)_2$ SCMs mainly came from Fe^{II}. This was in contrast to the $Mn^{II}Re^{IV}(CN)_2$ SCM.[5,6] The Re^{IV} ions only transmitted the exchange couplings between Fe^{II} ions and almost had no contribution to the barriers. Moreover, the total energy barriers for compounds **1**−**6** did not always increase as the Re^{IV}−Fe^{II} couplings increased, due to a decrease in the $(D_i - E_i)/J_1$ of Fe^{II}. Thus, to enlarge the energy barriers of SCMs, it is necessary to increase single-ion anisotropy, while simultaneously enhancing the intramolecular exchange interactions.

CONCLUDING REMARKS

In the Ising limit ($|D/J| \gg 4/3$), the expressions of Δ_ξ and Δ_A in terms of D, J, and S for SCMs are clear.[8] Billoni and coworkers also gave the expressions in the Heisenberg limit ($|D/J| \ll 4/3$).[27] In the intermediate region between the Ising and the Heisenberg limits ($|D/J| \approx 4/3$), however, the expressions of Δ_ξ and Δ_A in terms of D, J, and S are still unknown. Thus, we selected a series of $Fe^{II}Re^{IV}(CN)_2$ SCMs from the intermediate region, to obtain this correlation and investigate the origin of the magnetic anisotropy energy barriers using B3LYP and CASPT2 methods.

The six SCMs were divided into two groups by their $(D_i - E_i)/J$ and $2|E_i|/J$ values. The Δ_A values for compounds **1**−**3** (first group) were close to the magnetic anisotropic energy of a single Fe^{II}. The correlation energy Δ_ξ mainly came from the exchange interaction between Fe^{II} and the neighboring Re^{IV}, which was expressed as $2JS_{Re}S_{Fe}$. For compounds **4** and **5** (second group), the $(D_i - E_i)/J$ values of the Fe^{II} were less than 1; Δ_A for these compounds was estimated as $(D_i - E_i)S_{Fe}^2$. The correlation energy barrier Δ_ξ came from the exchange interaction between Fe^{II} and the central Re^{IV}, which was about $2JS_{Re}S_{Fe}(\cos 98.4 - \cos 180)$. Since there were two different Re^{IV}−Fe^{II} couplings in compound **6**, one unit cell of $Re^{IV}Fe^{II}$ was regarded as a domain wall. Δ_ξ of compound **6** was expressed as $4J''S_{Re1Fe1}S_{Re2Fe2}$, where J'' was the coupling constant of the neighboring unit cells of Re1Fe1 and Re2Fe2, and Δ_A was given by $D_{Re1Fe1}(S^2_{Re1Fe1} - 1/4)$. All the calculated Δ_ξ and Δ_A values were close to the experimental values, suggesting our approach was correct. This work needs to be validated in other SCMs.

The above results show that enhancing the Re^{IV}−Fe^{II} couplings did not always effectively increase the total energy barrier of $Fe^{II}Re^{IV}(CN)_2$ SCMs. To enlarge the total energy barrier, the single-ion anisotropy of Re^{IV} and Fe^{II} and Re^{IV}−Fe^{II} couplings must both be increased.

AUTHOR INFORMATION

Corresponding Authors

*E-mail: wangbw@pku.edu.cn. (B.W.W.)

*E-mail: gaosong@pku.edu.cn. (S.G.)

Notes

The authors declare no competing financial interest.

ACKNOWLEDGMENTS

This project is supported by the National Natural Science Foundation of China (90922033 and 21071008), the National Basic Research Program of China (2013CB933401, 2010CB934601), the Natural Science Foundation of Jiangsu Province of China (BK2011778), and China Postdoctoral Science Foundation funded project (2012M520104).

REFERENCES

(1) Caneschi, A.; Gatteschi, D.; Lalioti, N.; Sangregorio, C.; Sessoli, R.; Venturi, G.; Vindigni, A.; Rettori, A.; Pini, M. G.; Novak, M. A. *Angew. Chem., Int. Ed.* **2001**, *40*, 1760−1763.

(2) (a) Bogani, L.; Vindigni, A.; Sessoli, R.; Gatteschi, D. *J. Mater. Chem.* **2008**, *18*, 4750−4758. (b) Miyasaka, H.; Julve, M.; Yamashita, M.; Clérac, R. *Inorg. Chem.* **2009**, *48*, 3420−3437.

(3) Harris, T. D.; Bennett, M. V.; Clérac, R.; Long, J. R. *J. Am. Chem. Soc.* **2010**, *132*, 3980−3988.

(4) Feng, X. W.; Harris, T. D.; Long, J. R. *Chem. Sci.* **2011**, *2*, 1688−1694.

(5) Harris, T. D.; Coulon, C.; Clérac, R.; Long, J. R. *J. Am. Chem. Soc.* **2011**, *133*, 123−130.

(6) Feng, X. W.; Liu, J. J.; Harris, D.; Hill, S.; Long, J. R. *J. Am. Chem. Soc.* **2012**, *134*, 7521−7529.

(7) Gatteschi, D.; Sessoli, R.; Villain, J. *Molecular Nanomagnets;* Oxford University Press: Oxford, 2006.

(8) Coulon, C.; Miyasaka, H.; Clerac, R. *Struct. Bonding (Berlin)* **2006**, *122*, 163−206.

(9) Neese, F. *ORCA—An Ab Initio, Density Functional and Semiempirical Program Package,* Version 2.9.1; Max-Planck Institute for Bioinorganic Chemistry: Mülheim an der Ruhr, Germany, 2012.

(10) Becke, A. D. *J. Chem. Phys.* **1993**, *98*, 5648−5652.

(11) Becke, A. D. *Phys. Rev. A* **1988**, *38*, 3098−3100.

(12) Lee, C.; Yang, W.; Parr, R. G. *Phys. Rev. B* **1988**, *37*, 785−789.

(13) (a) Schafer, A.; Horn, H.; Ahlrichs, R. *J. Chem. Phys.* **1992**, *97*, 2571−2577. (b) Schafer, A.; Huber, C.; Ahlrichs, R. *J. Chem. Phys.* **1994**, *100*, 5829−5835.

(14) Perdew, J. P.; Burke, K.; Ernzerhof, M. *Phys. Rev. Lett.* **1996**, *77*, 3865−3868.

(15) (a) Neese, F. *J. Chem. Phys.* **2007**, *127*, 164112(1−9). (b) Pederson, M. R.; Khanna, S. *Phys. Rev. B* **1999**, *60*, 9566−9572. (c) Kortus, J.; Pederson, M. R.; Baruah, T.; Bernstein, N.; Hellberg, C. S. *Polyhedron* **2003**, *22*, 1871−1876. (d) Ribas-Arino, J.; Baruah, T.; Pederson, M. R. *J. Am. Chem. Soc.* **2006**, *128*, 9497−9505.

(16) Hess, B. A.; Marian, C. M.; Wahlgren, U.; Gropen, O. *Chem. Phys. Lett.* **1996**, *251*, 365−371.

(17) Maganas, D.; Sottini, S.; Kyritsis, P.; Groenen, E. J. J.; Neese, F. *Inorg. Chem.* **2011**, *50*, 8741−8754.

(18) Karlström, G.; Lindh, R.; Malmqvist, P. -Å.; Roos, B. O.; Ryde, U.; Veryazov, V.; Widmark, P.-O.; Cossi, M.; Schimmelpfennig, B.; Neogrady, P.; Seijo, L. *Comput. Mater. Sci.* **2003**, *28*, 222−239.

(19) Seijo, L.; Barandiarán, Z. *Computational Chemistry: Reviews of Current Trends;* World Scientific, Inc.: Singapore, 1999; Vol. 4, pp 55−152.

(20) Szabo, A.; Ostlund, N. S. *Modern Quantum Chemistry;* McGraw-Hill: New York, 1989.

(21) (a) Kahn, O.; Briat, B. *J. Chem. Soc., Faraday Trans.* **1976**, *72*, 268−281. (b) Girerd, J. J.; Journaux, Y.; Kahn, O. *Chem. Phys. Lett.* **1981**, *82*, 534−538.

(22) (a) Cauchy, T.; Ruiz, E.; Alvarez, S. *J. Am. Chem. Soc.* **2006**, *128*, 15722−15727. (b) Cano, J.; Costa, R.; Alvarez, S.; Ruiz, E. *J. Chem. Theory Comput.* **2007**, *3*, 782−788.

(23) Kahn, O. *Molecular Magnetism;* VCH: New York, 1993.

(24) Soo, H. S.; Sougrati, M. T.; Grandjean, F.; Long, G. J.; Chang, C. J. *Inorg. Chim. Acta* **2011**, *369*, 82−91.

(25) Harris, T. D.; Soo, H. S.; Chang, C. J.; Long, J. R. *Inorg. Chim. Acta* **2011**, *369*, 91−96.

(26) Barbara, B. *J. Magn. Magn. Mater.* **1994**, *129*, 79−86.

(27) Billoni, O. V.; Pianet, V.; Pescia, D.; Vindigni, A. *Phys. Rev. B* **2011**, *84*, 064415(1−16).